Protein Dynamics in Drug Combinations: a Linear Superposition of Individual-Drug Responses

Naama Geva-Zatorsky,[1,2] Erez Dekel,[1,2] Ariel A. Cohen,[1] Tamar Danon,[1] Lydia Cohen,[1] and Uri Alon[1,*]
[1]Departments of Molecular Cell Biology and Physics of Complex Systems, Weizmann Institute of Science, Rehovot 76100, Israel
[2]These authors contributed equally to this work
*Correspondence: urialon@weizmann.ac.il
DOI 10.1016/j.cell.2010.02.011

SUMMARY

Drugs and drug combinations have complex biological effects on cells and organisms. Little is known about how drugs affect protein dynamics that determine these effects. Here, we use a dynamic proteomics approach to accurately follow 15 protein levels in human cells in response to 13 different drugs. We find that protein dynamics in response to combinations of drugs are described accurately by a linear superposition (weighted sum) of their response to individual drugs. The weights in this superposition describe the relative impact of each drug on each protein. Using these weights, we show that one can predict the dynamics in a three-drug or four-drug combination on the basis of the dynamics in drug pairs. Our approach might eliminate the need to increase the number of experiments exponentially with the number of drugs and suggests that it might be possible to rationally control protein dynamics with specific drug combinations.

INTRODUCTION

Drug combinations are thought to be essential to treat multifactor diseases (Berenbaum, 1989; Greco et al., 1995; Keith et al., 2005). Much is known about the way drugs combine to affect biological outcome, such as cell death or proliferation (Lehár et al., 2007). Drug interaction experiments show synergy, independence, or antagonism of drug effects and are compared to classical pharmacological models such as Bliss independence (Bliss, 1939), Loewe additivity (Loewe, 1953), and more elaborate functions (Fitzgerald et al., 2006; Potti et al., 2006; Yeh et al., 2006; Garman et al., 2007; Lehár et al., 2007). The experimental study of multidrug combinations poses a well-known combinatorial problem, since the number of experiments grows exponentially with the number of drugs and doses measured.

Whereas drug effects on outcome are much studied, the effect of drug combinations on *protein dynamics* in the cell is much less investigated. Understanding the impact of drugs on each protein

is important in the context of a vision of a future medicine that controls protein dynamics precisely, using specific combinations of a large number of drugs. Imagine that the cell state can be described in a high dimensional space in which each axis is the level (or localization or activity) of one of the cells proteins (Figure 1). The goal is to guide the cell from a "sick state" to a "healthy state" in a rational manner (or, in the case of cancer, from a living cancer cell to a dead or quiescent cancer cell). This entails understanding the dynamical response of each protein to each drug at each dose, in the context of all possible combinations of the other drugs. To approach such rational control requires study of the degree to which protein dynamics in drug combinations can be understood.

To address this, we use a dynamic proteomics approach (Sigal et al., 2006; Cohen et al., 2008) to follow the dynamics of the expression level of a panel of proteins in individual living human cells at high temporal resolution and accuracy, as they respond to combinations of 13 drugs, including chemotherapeutic drugs, specific pathway inhibitors, and growth factors. We find that the dynamics of each protein in the presence of a drug combination is described accurately by a linear superposition (weighted sum) of the dynamics in the presence of each drug alone. The weights in this superposition are constant over time and depend on the drug dose. They describe the relative impact of each drug on each protein. We find that one can predict the dynamics in a multidrug combination on the basis of the dynamics in pairs of drugs. Extending this approach may allow understanding the vast space of multidrug and multidose combinations based on a relatively small number of two-drug measurements.

RESULTS

System for Measuring Protein Dynamics in Living Cells

To follow proteins in space and time in individual living cells, we used a dynamic proteomics approach (Sigal et al., 2006; Cohen et al., 2008). We employed a library of cell line clones, based on the H1299 human lung cancer cell line. In each clone, a different protein is tagged with yellow fluorescent protein (YFP), inserted as an exon in the chromosomal locus of the gene. The clone expresses a full-length fusion protein from its native chromosomal location under its endogenous regulation. Immunoblots
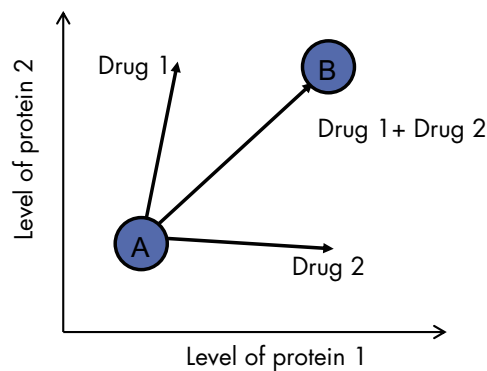
Figure 1. Schema for Rational Control of Cell State
Uses drug combinations to move cells from protein state A to protein state B. Each axis represents the level, location, modification or activity of one protein (or other component or process). In this study, we focus on protein level (expression) dynamics. Only two axes are drawn, out of the many thousands representing all cell proteins.

on a subset of these clones indicated that 80% of the tagged proteins serve as accurate markers for the dynamics of the endogenous protein (Cohen et al., 2008). The present library includes about 1400 different tagged proteins. The clones are all tagged with a second red fluorescent marker that enables automated image analysis (Cohen et al., 2008).

For this study, we selected 15 proteins that represent different aspects of cell biology (see Table S3, part a, available online).

These include representatives from systems such as the ribosome, oxidative stress, DNA repair, metabolism, cytoskeleton, and apoptosis. The proteins localize to different cell compartments, including the nucleus, cytoplasm, and nucleoli. The dynamics of each protein in the presence of drugs was monitored by time-lapse microscopy under incubated conditions in multi-well plates as described in Cohen et al. (2008) (see the Experimental Procedures). Dynamics of the fluorescence of tagged protein for each cell was obtained by automated image analysis. The dynamics presented are the average of 200–400 individual cell dynamical profiles, taken from two to four repeated movies with four fields of view in the same well for each movie. Day-day reproducibility of the dynamics was better than 10% (RMS error).
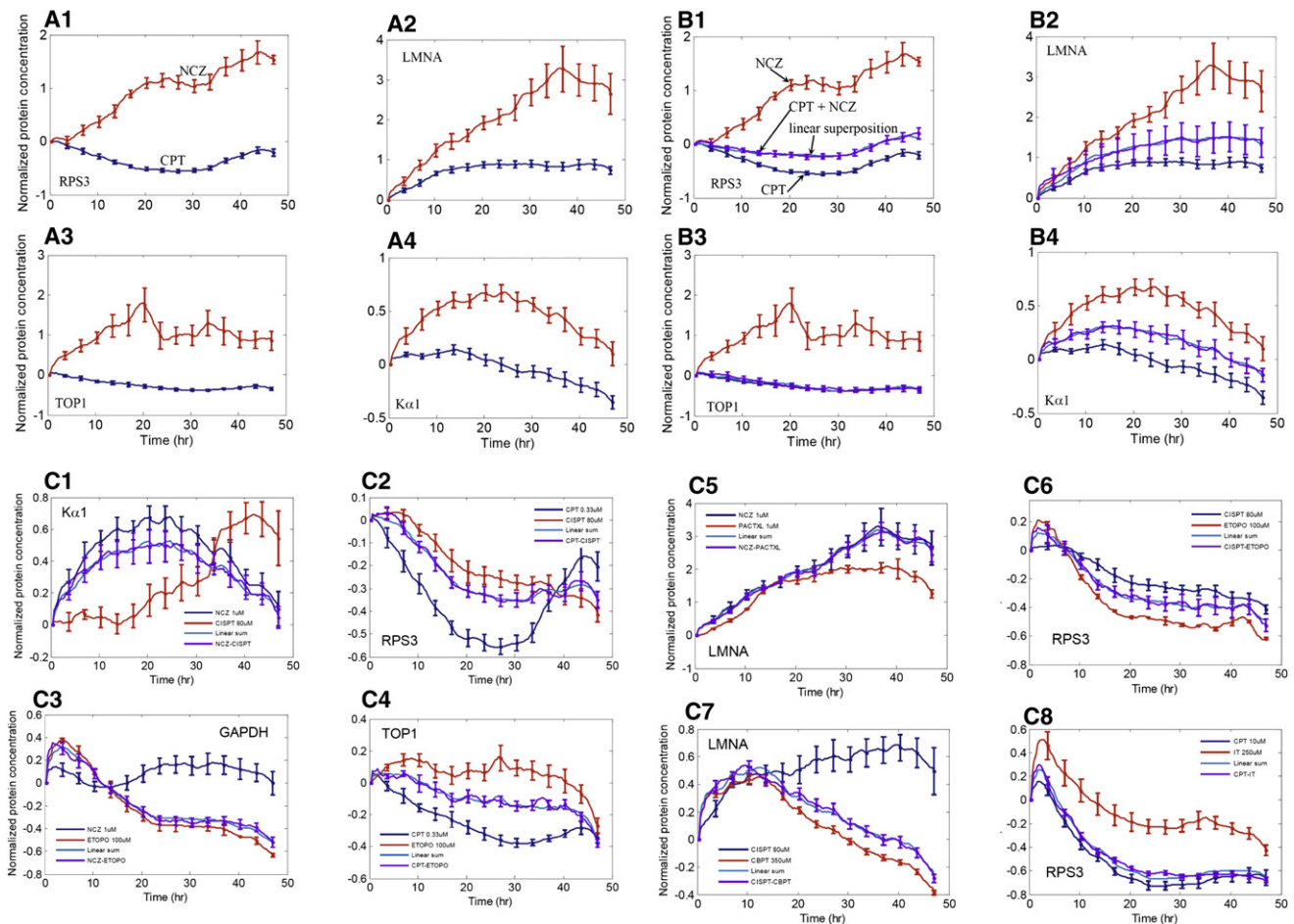
Proteins Show Different Dynamics under Each Drug

We chose 13 drugs including chemotherapy agents, pathway inhibitors, and growth factors (Table S3, part b). These drugs have diverse antagonistic or synergistic interactions when assayed for cell death using neutral red (Table 1). For example, etoposide (ETOPO) combined with camptothecin (CPT) shows synergism, in the sense of enhanced cell killing relative to Bliss independence (in which each drug kills a fraction of the cells independently of the other). In contrast, ETOPO combined with Nocodazole (NCZ) shows reduced killing (antagonism).

We tested the dynamics of the 15 proteins with these drugs at equi-lethal concentrations (for some drugs, only a subset of the proteins was tested). We find that each protein shows different

Table 1. Summary of Survival after Chemotherapy Drug Combination Treatment

Combination	Dose (μM)	Survival[a] (Measured)	Survival[b] (Bliss Independence)	Interaction[c]
CPT	0.33	0.75 (±0.04)[d]	*	*
CPT	0.01	0.95 (±0.11)	*	*
CisPt	80	0.90 (±0.15)	*	*
CisPt	800	0.52 (±0.08)	*	*
CisPt	0.8	1.00 (±0.10)	*	*
NCZ	1	0.47 (±0.06)	*	*
Etopo	100	0.29 (±0.03)	*	*
CPT/CisPt	0.33/80	0.68 (±0.08)	0.68 (±0.12)	additive
CPT/CisPt	0.33/800	0.20 (±0.02)	0.39 (±0.06)	synergistic
CPT/NCZ	0.33/1	0.80 (±0.10)	0.35 (±0.05)	antagonistic
NCZ/CisPt	1/80	0.73 (±0.07)	0.42 (±0.09)	antagonistic
NCZ/CisPt	1/800	0.37 (±0.02)	0.24 (±0.05)	antagonistic
Etopo /CPT	100/0.33	0.08 (±0.02)	0.22 (±0.03)	synergistic
Etopo /CisPt	100/80	0.27 (±0.02)	0.27 (±0.05)	additive
Etopo /NCZ	100/1	0.44 (±0.06)	0.14 (±0.02)	antagonistic
CPT/NCZ/CisPt	0.33/1/80	0.69 (±0.09)	0.32 (±0.07)	antagonistic
CPT/CisPt/Etopo	0.33/80/100	0.08 (±0.02)	0.20 (±0.04)	synergistic
CPT/NCZ/CisPt/Etopo	0.33/1/80/100	0.10 (±0.06)	0.09 (±0.02)	additive

See also Figure S6.
[a] Surviving cells in response to the indicated drugs and their combinations as was measured by neutral red assay (see the Experimental Procedures).
[b] The predicted survival based on Bliss independent model (see the main text).
[c] Synergism is defined when the actual measured number of viable cells is lower than the Bliss model. Antagonism is for the opposite, and additive is when measured and Bliss viability match within their errors.
[d] Standard errors from six repeats are numbers in parentheses.

Figure 2. Protein Dynamics in Drug Combinations Can Be Described as a Linear Superposition of the Dynamics under Single Drugs Applied Separately

(A) Proteins respond differently to each drug. Shown are protein fluorescence levels as a function of time after the addition of drugs at time t = 0. Protein fluorescence levels P(t) are normalized to initial level at time of drug addition *P(0)*, as follows *(P(t)-P(0))/P(0)*. Ribosomal protein RPS3 (1), nuclear lamina protein LMNA (2), TOP1 (3), and Kα1 (alpha tubulin) with 0.33 μM CPT (blue) and 1 μM NCZ (red) (4) are shown. Error bars represent the standard errors of three or more independent experimental repeats.

(B) Dynamics in drug pair is a linear superposition of the dynamics in each drug alone. Shown are same proteins and drugs as in (A). Dynamics in the presence of both drugs is in purple. The linear superposition is in light blue. Error bars represent the standard errors of three or more independent experimental repeats.

(C) Dynamics in drug pair is a linear superposition of the dynamics in each drug alone. Proteins and drug combinations are indicated. Dynamics in the presence of both drugs is in purple, linear superposition is in light blue. Error bars represent the standard errors of three or more independent experimental repeats.

See also Figures S1, S2, S3, and S4 and Tables S1 and S2.

dynamics for each drug. For example, ribosomal protein RPS3 levels rise under NCZ, but decrease under CPT (Figure 2A, part 1). Thus, drugs that all result in cell death still have different effects on each of the proteins (Figure 2A).

Dynamics under Two-Drug Combinations Is a Linear Superposition of Single-Drug Dynamics

We next tested the dynamics of the 15-protein panel in combinations of drug pairs. Here, we mixed together the same doses as used for the single-drug dynamics. We tested a total of 19 combinations of the 13 drugs. We find that in 12 of the 13 drugs (the exception is PI3K inhibitor, discussed below) the dynamics in drug pairs can be described to within experimental error by

a weighted sum of the dynamics in the presence of each drug alone (Figures 2B and 2C). Thus,

$$P_{i+j}(t) = w_i \, P_i(t) + w_j \, P_j(t).$$

Here, P_{i+j} is the protein level in the combination of drugs *i* and *j*, P_i and P_j are the levels in each drug alone. Protein levels are normalized to the initial protein level before the drugs are added, *P(t) = (P(t)-P(0))/P(0)*. Note that the weights w_i and w_j are *constant over time*. In other words, measurement of each drug alone, and the combination at a single time point to estimate the two weights w_i and w_j, is enough to predict the dynamics of the combination at all time points in the experiment.
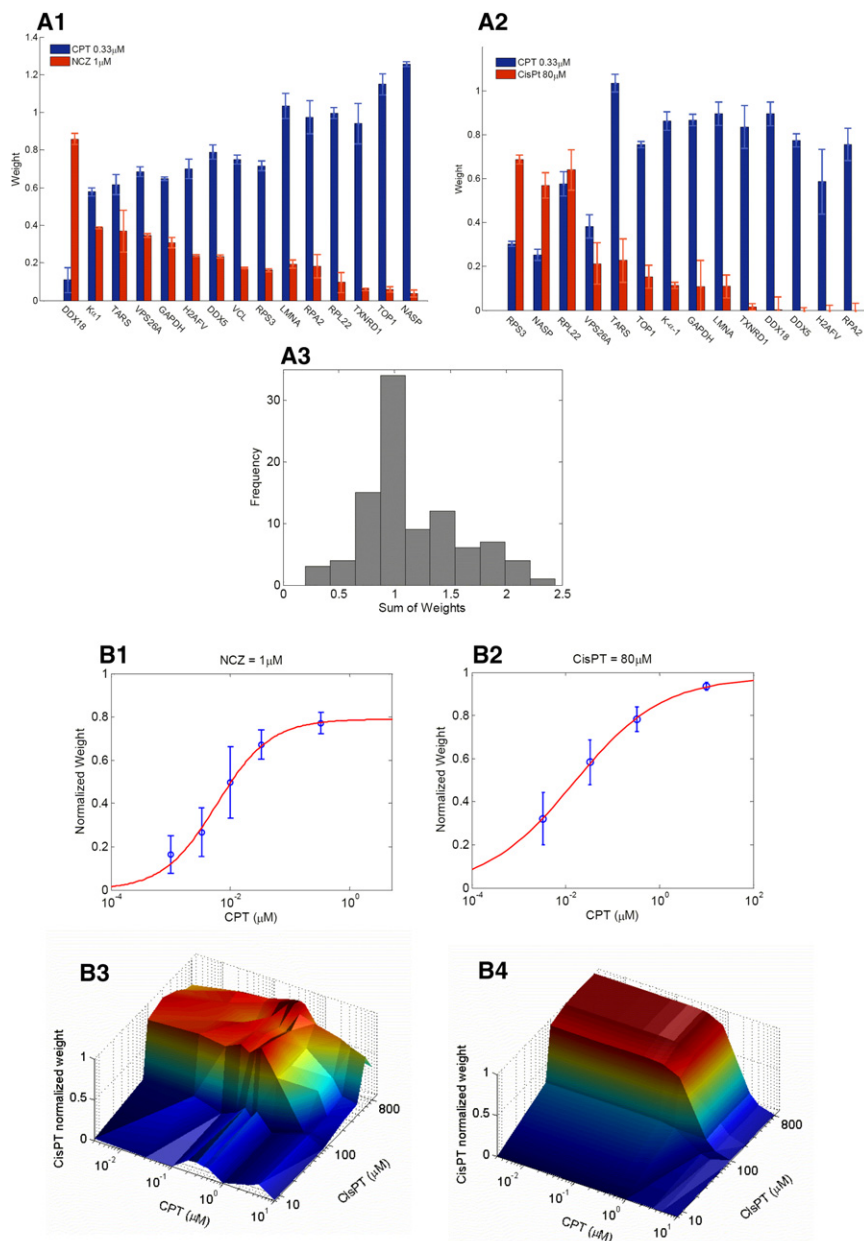
Figure 3. The Linear Superposition Weights Are Specific to Each Protein, Indicate Dominance of Drugs, and Increase with Drug Dose

(A) Weights indicate effect of each drug for each protein. Shown are weights (blue for CPT 0.33 μM and red for NCZ 1 μM) for proteins in the combination of CPT and NCZ (1). CPT dominates NCZ for most proteins (DDX18 is an exception). Weights (blue for CPT 0.33 μM and red for CisPt 80 μM) for proteins in the combination of CPT and CisPt are shown in (2). CPT dominates CisPt for most proteins. Error bars are the 95% confidence range of linear fit. (3) shows a histogram of the sum of weights of individual proteins in all experiments is centered around 1.

(B) Weights for a given drug increase with its dose. (1) and (2) show the mean weight over different proteins at different CPT concentrations and at a constant NCZ concentration of 1 μM (1) and a constant CisPt concentration of 80 μM (2). Error bars represent the STDs of the weights of different proteins. The solid line is a Hill function with $n = 1 \pm 0.6$ and $K = 7 \pm 5$ nM (1), and $n = 0.5 \pm 0.3$ and $K = 15 \pm 7$ nM (2). Error bars indicate standard errors. Weights for LMNA as a function of the doses of CisPt and CPT are shown in (3). The CisPt weight is shown, which increases with CisPt dose and decreases with CPT dose. This is well fit as a product of two Hill-like functions one increasing with with $n_1 = 8 \pm 7$, $K_1 = 85 \pm 7$ μM, and the other decreasing with $n_2 = 1 \pm 0.7$ and $K_2 = 2 \pm 2$ μM (4). See also Figures S3, S4, and S5 and Table S2.

The weights are specific for each protein (Figure 3A, parts 1 and 2), and in most cases they add up to approximately one: $w_i + w_j \sim 1$ (Figure 3A, part 3). Thus, the dynamics in the present two-drug combinations tend to lie between the dynamical curves of each drug alone, similar to a weighted average of the two curves. Such superposition is somewhat surprising. In principle, one may have expected other effects; for example, a protein response that exceeds both single drug responses, such as would result if the two dynamics were purely additive (with $w_i = w_j = 1$).

As a statistical test of the superposition phenomenon, we performed a data shuffling test. In this test, we attempted to describe the dynamics of a protein in two-drug combinations by means of a weighted sum of the single drug dynamics of *other*

proteins (Figure S1). We find that the error of the best-fit superposition in this shuffling approach is always higher than the error that results when describing each protein as a superposition of its own single-drug dynamic profiles (p < 0.001).

As a further test, we used principle component analysis (PCA) (Pearson, 1901; Jolliffe, 2002) to ask to what extent the two-drug dynamics are a linear combination of the single-drug dynamics. If the measured combination P_{i+j} is a pure linear combination of the individual-drug dynamics P_i, P_j, then PCA over the three vectors P_i, P_j, and P_{i+j} would result in only two components that are larger than zero and a third component that is equal to zero. Application of PCA to all 15 proteins results in 99.5% of the variability in the two first principle components, leaving only a 0.5% effect not explained by linear superposition (Figures S1A–S1F).

Some trends in the weights can be seen, where certain drugs seem to have larger weights than others. We find that the weights for CPT for most proteins are larger than those for NCZ and similarly larger than the weights for CisPt (Figure 3A, parts 1 and 2). This means that the combination of either NCZ or CisPt with CPT at the present doses leads to dynamics that are dominated by CPT. In particular, the CPT drug target, TOP1, shows

A

B
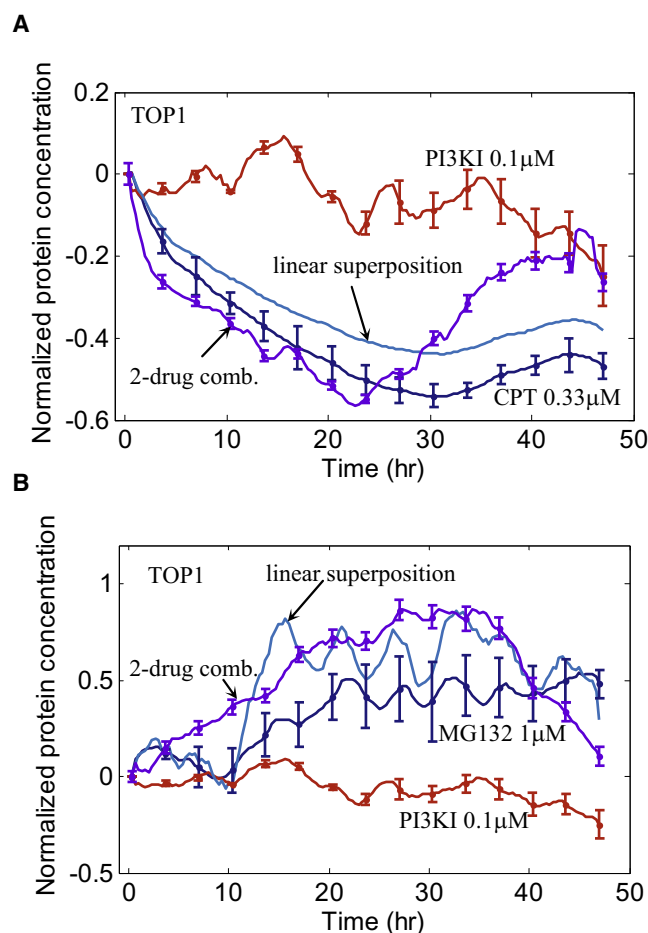
Figure 4. The PI3-Kinase Inhibitor, PI3KI, Does Not Show Linear Superposition

Dynamics of TOP1 in the combinations CPT (0.33 μM) and PI3KI (0.1 μM) (A) and MG132 (1 μM) and PI3KI (0.1 μM) (B) are not well described by a linear superposition (best fit linear superposition is in light blue). Error bars represent the standard errors of three or more independent experimental repeats. See also Table S1.

dynamics completely dominated by CPT, with weight close to one for CPT and nearly zero for the other drug in the pair. The dominance of CPT does not apply however to all proteins: an exception is the protein DDX18, in which NCZ dominates CPT. This may point to the pathway-specific impact of each drug.

Overall, about 20% of the cases we tested showed strong dominance by one drug in a drug pair (three out of 15 cases showed dynamics more than 90% dominated by one of the two drugs).

Weights for Each Drug Increase with Drug Dose

We also tested the effects of varying the drug dose. We find that the linear superposition principle applies across drug concentrations. The resulting weights for a given drug are an increasing function of its dose (Figure 3B, parts 1 and 2). For example, when CPT levels are reduced from 330 nM to 3.3 nM, it is no longer dominant over NCZ for most proteins. The weights as

a function of dose x are reasonably described by Hill-like functions, $w_i(x) = w_{max} \, x^n/(K^n+x^n)$. The halfway point K depends on the dose of the other drug in the pair.

We extensively tested the superposition hypothesis in the case of the protein LMNA, in 96 different dose combinations of CPT and CisPt, using a 96-well assay in the microscope. We find that linear superposition accurately describes the dynamics in all dose combinations. The weights in each dose combination can be represented in a two-dimensional map (Figure 3B, part 3), and are well fit by the product of two Hill-like functions (Figure 3B, part 4). Thus, the weight for CisPt in the presence of CPT is $w_1(x,y) = h_1(x) \cdot h_2(y)$, where x is the CisPt dose and y is the CPT dose. Here, h_1 is a Hill functions of x, $h_1(x) = x^{n_1}/x^{n_1} + K_1^{n_1}$, and h_2 is a decreasing Hill function of y, $h_2(y) = K_2^{n_2}/y^{n_2} + K_2^{n_2}$. Similar findings were obtained with 96 combinations of CPT and NCZ.

No Linear Superposition Is Found with PI3K Inhibitor

One drug does not seem to show linear superposition with other drugs, the PI3K inhibitor, Wortmanin. Addition of this compound to other drugs seems to result in dynamics that can not be well described as a weighted sum of the two single-drug dynamics (Figures 4A and 4B). We could not find a compelling reason why this drug behaves differently from the others in the present study.

Adding a Drug to Itself

An additional test case is when a drug is combined with itself. This can be considered as a limiting case in which the two drugs in a cocktail are one and the same. One can imagine situations where, for example, the dynamical profile of a drug at dose x is not a weighted sum of its two dynamical curves at dose $x/2$. We tested this for three of the drugs, CPT, ETOPO, and CisPt. We find that for most concentrations, linear superposition holds to excellent approximation even when adding a drug to itself (Table S1 and Figure S2).

Linear superposition can be mathematically shown to hold true when adding a drug to itself, if the drug has a dose response that can be separated into a product of a dose-dependent function and a time-dependent one, in the following way: $P(D,t) = h_1(t) + h_2(t) \cdot g(D)$, where D is the dose and t the time (see the Extended Results, "Adding a Drug to Itself"). The drugs presently tested seem to have a dose-response that shows such a separability feature. It is conceivable, however, that other drugs have a nonseparable interplay between dose and temporal response profiles, so that linear superposition of the drug with itself will not hold.

Dynamics in Three-Drug and Four-Drug Combinations Can Be Predicted on the Basis of Two-Drug Dynamics

We next tested combinations of three drugs, CPT (0.33 μM) + CisPt (80 μM) + NCZ (1 μM) (Table S1) and CPT (0.3 μM) + CisPt (80 μM) + ETOPO (100 μM) (Figure 5A and Table S1), and a combination of all four drugs CPT (0.33 μM) + CisPt (80 μM) + ETOPO (100 μM) + NCZ (1 μM) (Figure 5B and Table S1). We find that, as in the two-drug case, the dynamics are a linear superposition of the single-drug dynamics. Superposition captures multidrug dynamics extremely well (the fit lies within

A1

A2

A3

A4

B1

B2

B3

B4

B5
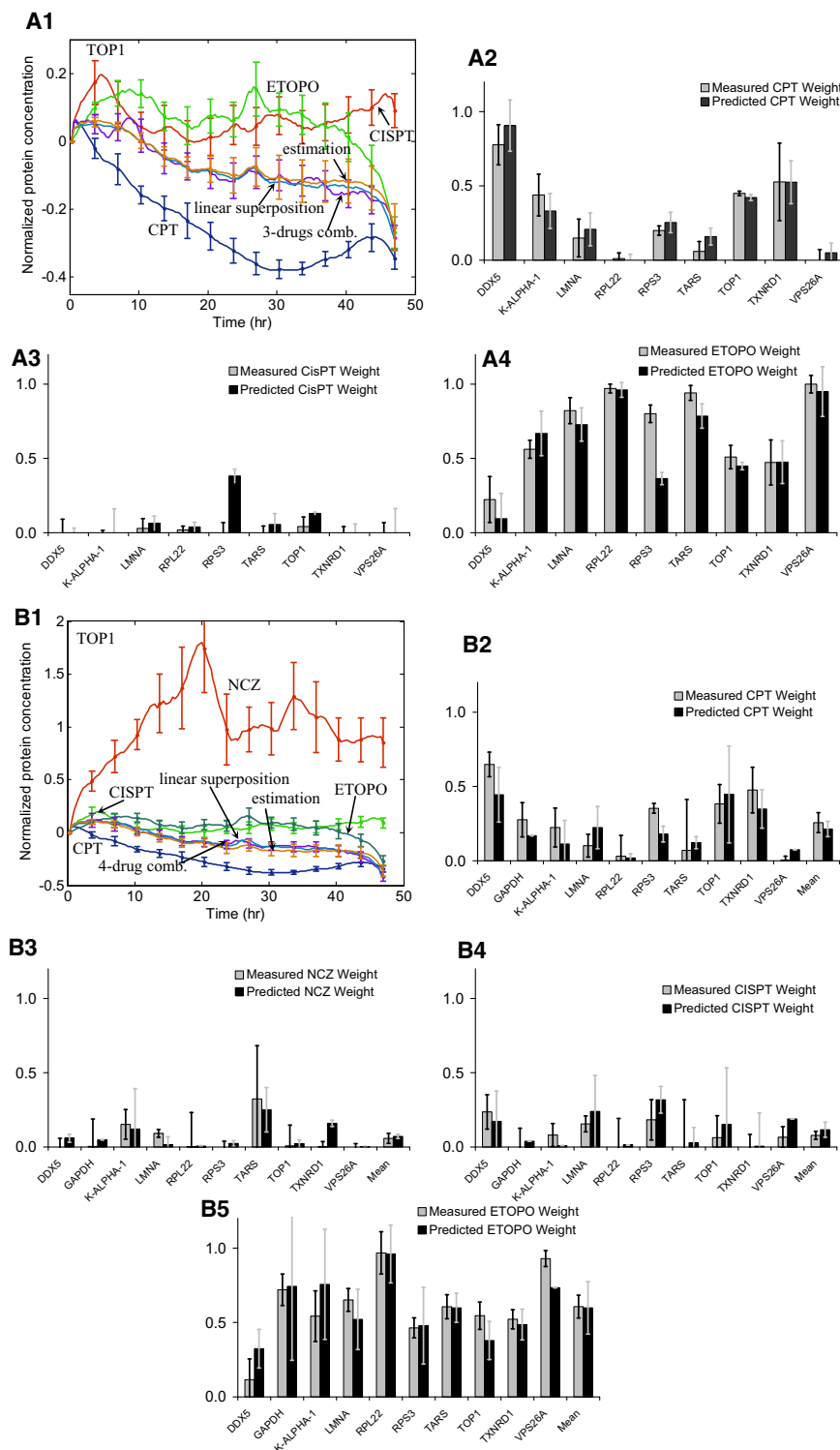
Figure 5. Dynamics in Three-Drug and Four-Drug Combinations Can Be Predicted on the Basis of Two-Drug Dynamics

(A) Dynamics in a combination of three drugs is a linear superposition of single-drug dynamics and can be predicted based on two-drug weights. Dynamics of TOP1 under CPT (0.33 μM) (blue), CisPt (80 μM) (red) and ETOPO (100 μM) (green), and in a combination of all three (purple), is well described by a linear superposition (light blue) and by the estimated response on the basis of two-drug combination (orange) (1). Error bars represent the standard errors of three or more independent experimental repeats. Best-fit (gray) and predicted (black) weights of CPT (2), CisPt (3), and ETOPO (4) for the proteins are shown. Error bars are the 95% confidence range of linear fit. Dynamics for all proteins tested is shown in Table S1. See also Figure S5.

(B) Dynamics in a combination of four drugs is a linear superposition of single drug dynamics and can be predicted on the basis of two-drug weights. Dynamics of TOP1 under CPT (0.33 μM) treatment (blue), NCZ (1 μM) (red), CisPt (80 μM) (green), ETOPO (100 μM) (dark green), and in a combination of all four (purple) is well described by a linear superposition (light blue) and by the estimated response based on two-drug combination (orange) are shown in (1). Error bars represent the standard errors of three or more independent experimental repeats. Best-fit (gray) and predicted (black) weights of CPT (2), NCZ (3), CisPt (4), and ETOPO (5) for individual proteins are shown. Error bars are the 95% confidence of linear fitting. See also Table S1.

that if the linear superposition principle holds for three drugs

$$P_{i+j+k} = w_i^{(ijk)}P_i + w_j^{(ijk)}P_j + w_k^{(ijk)}P_k$$

and for each of the three different pair combinations

$$P_{i+j} = w_i^{(ij)}P_i + w_j^{(ij)}P_j,$$

then one has enough equations to solve for the three-drug weights on the basis of the two-drug weights (see the Extended Results, "Derivation of the Prediction Equations for Three and More Drugs," and Table S1). Here, w_i^{ij} denotes the weight of drug i in the presence of drugs $i+j$, and for the purpose of the present calculation weights are normalized to sum up to one. The resulting formula for three-drug weights based on the two-drug weights is

$$w_i^{(ijk)} = \frac{w_i^{(ik)} - w_i^{(ik)}w_j^{(jk)}}{1 - w_i^{(ik)}w_j^{(jk)}}.$$

the bounds of the experimental error) and is highly significant in data shuffling tests ($p < 10^{-4}$). The weights are again specific to each protein and sum up to approximately one.

We hypothesized that the three-drug weights can be predicted based on the two-drug weights. To see this, note

The same reasoning can be extended to four drugs and more. The corresponding formula for N-drug weights based on (N−1)-drug weights is

$$w_i^{(1..N)} = \frac{w_i^{(\neq j)} - w_i^{(\neq j)} w_j^{(\neq i)}}{1 - w_i^{(\neq j)} w_j^{(\neq i)}},$$

where (≠j) means all drugs but j. This results in one equation for each choice of $j \neq i$, a total of N−1 equations. These equations can be solved starting from two-drug weights until one reaches N-drug weights. We estimated the weights in the four-drug combinations by averaging over the predictions given by these equations. We find that the predicted weights agree very well with the best-fit weights for most proteins (Figure 5 and Figure S5): correlation between best-fit and predicted weights is R = 0.92, p < 10^−15. Thus, knowledge of two-drug weights seems to provide a good estimate for dynamics in three- and four-drug combinations.

DISCUSSION

We studied the effects of drug combinations on the dynamics of endogenously tagged proteins in living human cells. We find that each protein responds differently to each drug. The protein dynamics under a combination of drugs is well described in most cases by a linear superposition (a weighted sum) of the dynamics under each drug alone. The weights are specific to each protein and are dose dependent and constant over time. They tend to sum up to approximately one. The linear superposition principle seems to carry over also to three- and four-drug combinations, where the dynamics can be predicted on the basis of two-drug measurements. This suggests that, at least for these drugs and cells, protein level dynamics might be rationally controllable on the basis of a simple superposition principle.

The present approach offers a way to bypass the combinatorial explosion problem of research on drug combinations. If drugs interacted to affect protein levels in a complex nonlinear way, one would need a separate experiment to understand each drug-dose combination. Thus, to explore all possible combinations requires a number of experiments that grows exponentially with the number of drugs and doses. A potential way to bypass this challenge lies in the finding that three- and four-drug dynamics can be predicted on the basis of two-drug dynamics. If this may be extended to other proteins, drugs and cells, the present approach can reduce the combinatorial explosion problem inherent in understanding multidrug combinations.

To make this reasoning explicit, note that measurement of all combinations of N drugs at k dose levels requires k^N experiments. In contrast, measurement of single and double drug mixes requires far fewer experiments, $k^2N(N-1)/2+Nk$. For N = 10 drugs and k = 8 doses, this means about 10^9 experiments for all combinations, and only about 3000 measurements (31 96-well experiments) to cover all single-drug and drug-pair dynamics. To measure all combinations of 100 drugs, each either present or absent in a cocktail, requires $2^{100} \sim 10^{30}$ experiments, but only about 5000 experiments to cover all pairs.

Thus, if the superposition principle applies beyond the present system, relatively few drug-pair measurements may allow one to computationally navigate the high-dimensional space of drugs and doses and to find an optimal drug cocktail (Jonker et al., 2005). It is expected that the predictions will only be approximate, but they can serve as a guide to relevant regions of drug-dose space that would otherwise be prohibitively difficult to find.

Why are the effects of drugs on protein dynamics linearly superposable? Why does a small set of constants, the weights, describe the relations between single- and multiple-drug behavior at all time points? This is a fascinating avenue for future research. One way to obtain such linear superposition is by describing protein responses as a linear perturbation around the steady-state of a nonlinear system (Strogatz, 2001; Thattai and van Oudenaarden, 2001; Tegner et al., 2003; Prill et al., 2005). This does not seem to explain most of the cases considered in this study, because linear perturbations apply only to small variations, whereas the present experiments show rather large dynamical movements.

Future work can test when superposition holds and breaks down, and, more generally, how the structure of cell circuits (Alon, 2006) affects protein dynamics in response to drugs and drug combinations. (di Bernardo et al., 2005; Lehár et al., 2007). At present, we do not have a mechanistic explanation for superposition. Further experimental and theoretical work will be required to answer such questions.

We hope that the present study is a step in the direction of a future medicine that produces precise biological outcome by rationally controlling the dynamics of proteins in cells. Drug combinations based on the superposition principle can perhaps aim toward alleviating unwanted side effects (using drugs to cancel out each other's unwanted effects on specific proteins), and improving efficacy.

EXPERIMENTAL PROCEDURES

Fluorescently Tagged Protein Clones
All clones in this study are from the LARC library, in which proteins were fluorescently tagged in their endogenous chromosomal locus under their endogenous regulation, by CD tagging, as described (Sigal et al., 2006; Sigal et al., 2007; Cohen et al., 2008). Clones are based on H1299 non-small-cell lung carcinoma cells and were described Cohen et al. (2008).

Tissue Culture Media
Cells were grown in RPMI 1640 supplied with (+) L-Glutamine (GIBCO, catalog number 21875) medium supplemented with 10% Fetal Calf Serum (certified fetal bovine serum, membrane filtered, Biological Industries, catalog number 04-001-1A) and 0.05% Penicillin-Streptomycin antibiotics (Biological Industries, catalog number 03-031-1B). Cells were grown in incubators at 37°C and 8% CO_2.

Drugs
Cisplatinum (P4394 Sigma) was dissolved in DMSO (hybri-max, D2650 Sigma) giving a stock solution of 100 mM; Nocodazole (M1404, Sigma) was dissolved in DMSO giving a stock solution of 33.2 mM; and Camptothecin (CPT, C9911 Sigma) and Etoposide (E1383 Sigma) were dissolved in DMSO giving a stock solution of 10 mM. Human recombinant EGF was reconstituted in 10 mM acetic acid containing 0.1% BSA to a final concentration of 10 μg/ml; HGF (Calbiochem, catalog number 375228) was dissolved in sterile PBS to a final concentration of 2 μg/ml (26.7 nM). MAPK inhibitor (U0126, Calbiochem, catalog number 662005) was dissolved in DMSO to a final concentration of 5 mM. In each experiment, drug was diluted to the desired concentration in

transparent growth medium (RPMI 1640, 0.05% Penicillin-Streptomycin antibiotics, 10% FCS, with L-Glutamine, lacking riboflavin and phenol red, Bet Haemek, Biological Industries, catalog number 06-1100-26-1A). Normal transparent growth medium (2 ml, without the drug) was replaced by the diluted drug (2 ml medium with the final desired concentration of each drug) under the microscope after at least one round of images without the drug (at least one image per each field of view was taken before drug addition).

Viability Assay

Cell viability was determined by neutral red accumulation (Fluka Chemie, catalog number 72210, Buchs, Switzerland), (Zhang et al., 1990) as follows: after 48 hr incubation (37°C, 8% CO_2) with drugs (or no drugs as control), 100 μl neutral red reagent (diluted 1:100 in growth medium) was added to cells for 35 min incubation. Neutral red buffer was washed and fixation buffer (1% $CaCl_2$, 0.5% formaldehyde) was added. For extraction of the remaining cells, extraction buffer (1% glacial acetic acid, 50% ethanol) was added. Cells were shaken for 10 s, and optical density (570 nm) was read by an ELISA reader (BIO-RAD Model 680 Microplate Reader). After subtraction of assay blanks (wells with no cells), net optical density was computed as the average value of six replicate determinations. Cell survival was calculated as the percentage of the dye accumulated in the untreated controls.

Time-Lapse Microscopy

Time-lapse movies were obtained at 20× magnification. Four automated microscopes were used, three inverted fluorescence microscopes from Leica (DMIRE2 and DMI6000B) and one from Olympus (modified IX71). All microscopes included live-cell environmental incubators maintaining 37°C (37-2 digital and Heating unit, PeCon, Germany, Leica #15531719) humidity and 8% CO_2 (PeCon, Germany #0506.000-230, Leica #11521733) and automated stage movement control (Corvus, ITK, Germany); the stage was surrounded by a custom enclosure to maintain constant temperature, CO_2 concentration, and humidity. Transmitted and fluorescence light paths were controlled by electronic shutters (Uniblitz, model VMM-D1, Rochester, NY); fluorescent light sources were Mercury short arc lamp HXP and Mercury HBO100 (OSRAM, Germany). Cooled 12 and 14 bit CCD cameras were used, QImaging, (RETIGA-S&V, Fast 1394, RET-SRV-F-M-12-C, Canada), CoolSNAP (Roper Scientific HQ, photometrics), ORCA-ER (C4742-95-12ERG, Hamamatsu photonics K.K, Japan), and iXon (Andor technology). The filters used were from Chroma Technology: on the Leica systems, single-channel filters were YFP (500/20 nm excitation, 515 nm dichroic splitter, and 535/30 nm emission, Chroma #41028) and mCherry Red (575/50 nm excitation, 610 nm dichroic splitter, and 640/50nm emission, Chroma #41043) and on the Olympus Dual channel dichroic with excitation and emission filters mounted on fast filter wheels (Chroma set 490/20x, 577/25x, 535/30 m, 632/60 m). The Leica system hardware was controlled by ImagePro5 Plus software (Media Cybernetics), which integrated time-lapse acquisition, stage movement, and software-based autofocus (adjusted in our lab). The Olympus system integration and fast laser autofocus was from Idea Bio-Medical (Rehovot, Israel).

Cells were grown and visualized in 12-well optical glass-bottom plates (Mat-Tek cultureware, Microwell plates-uncoated, part number P12G-0-14-F, lot number TK0289) or optical bottom 96-well plates (Nunc, 164588), both coated with 10 μM fibronectin 0.1% (solution from bovine plasma, Sigma, catalog number F1141) diluted 1:100 in Dulbecco's phosphate-buffered saline (PBS; Sigma, catalog number D8537). In order to reduce background fluorescence, cells were grown in RPMI 1640 lacking riboflavin and phenol red (Beit Haemek, Biological Industries, catalog number 06-1100-26-1A) supplemented with L-Glutamine, 10% fetal calf serum (certified fetal bovine serum, membrane filtered, Biological Industries, 04-001-1A), and 0.05% Penicillin-Streptomycin antibiotics (Biological Industries, catalog number 03-031-1B). For each well, time-lapse movies were obtained at four fields of view. Each movie was taken at a time resolution of 20 min and was filmed for at least 2 days (over 140 time points). Each time point included transmitted light image (phase contrast) and two fluorescent channels (red and yellow).

Image Analysis of Time-Lapse Movies

We used the image analysis software described in Cohen et al. (2008). The main steps in this software include background correction (flat field and

background subtraction), segmentation, cell tracking, and automated identification of cell phenotypes (mitosis and cell death). No significant bleaching was observed (on average less than 3% over the duration of the experiment). Cell and nuclei segmentation was based on the red fluorescent images of the red tagged protein found in all clones, localized to the cytoplasm and nucleus, with intensity which is very uniform across cells and clones. Segmentation used global image threshold (Otsu, 1979) and seeded watershed segmentation. Seeds were obtained by smoothening of the red intensity image and use of nuclei as cell seeds. Tracking was performed by analysis of the movie from end to start and linking of each segmented cell to the cell in the previous image with the closest centroid. Automated cell death identification algorithm utilized the morphological changes correlated with dying cells.

SUPPLEMENTAL INFORMATION

Supplemental Information includes Extended Results, six figures, and three tables and can be found with this article online at doi:10.1016/j.cell.2010.02.011.

REFERENCES

Alon, U. (2006). An Introduction to Systems Biology: Design Principles of Biological Circuits (London: Chapman & Hall/Crc).

Berenbaum, M.C. (1989). What is synergy? Pharmacol. Rev. 41, 93–141.

Bliss, C. (1939). The toxicity of poisons applied jointly. Ann. Appl. Biol. 26, 585–615.

Cohen, A.A., Geva-Zatorsky, N., Eden, E., Frenkel-Morgenstern, M., Issaeva, I., Sigal, A., Milo, R., Cohen-Saidon, C., Liron, Y., Kam, Z., et al. (2008). Dynamic proteomics of individual cancer cells in response to a drug. Science 322, 1511–1516.

di Bernardo, D., Thompson, M.J., Gardner, T.S., Chobot, S.E., Eastwood, E.L., Wojtovich, A.P., Elliott, S.J., Schaus, S.E., and Collins, J.J. (2005). Chemogenomic profiling on a genome-wide scale using reverse-engineered gene networks. Nat. Biotechnol. 23, 377–383.

Fitzgerald, J.B., Schoeberl, B., Nielsen, U.B., and Sorger, P.K. (2006). Systems biology and combination therapy in the quest for clinical efficacy. Nat. Chem. Biol. 2, 458–466.

Garman, K.S., Nevins, J.R., and Potti, A. (2007). Genomic strategies for personalized cancer therapy. Hum. Mol. Genet. 16 Spec No. 2, R226–R232.

Greco, W.R., Bravo, G., and Parsons, J.C. (1995). The search for synergy: a critical review from a response surface perspective. Pharmacol. Rev. 47, 331–385.

Jolliffe, I.T. (2002). Principle Component Analysis (Aberdeen, UK: Springer Series in Statistics).

Jonker, D.M., Visser, S.A., van der Graaf, P.H., Voskuyl, R.A., and Danhof, M. (2005). Towards a mechanism-based analysis of pharmacodynamic drug-drug interactions in vivo. Pharmacol. Ther. 106, 1–18.

Keith, C.T., Borisy, A.A., and Stockwell, B.R. (2005). Multicomponent therapeutics for networked systems. Nat. Rev. Drug Discov. 4, 71–78.

Lehár, J., Zimmermann, G.R., Krueger, A.S., Molnar, R.A., Ledell, J.T., Heilbut, A.M., Short, G.F., 3rd, Giusti, L.C., Nolan, G.P., Magid, O.A., et al. (2007).

Chemical combination effects predict connectivity in biological systems. Mol. Syst. Biol. *3*, 80.

Loewe, S. (1953). The problem of synergism and antagonism of combined drugs. Arzneimittelforschung *3*, 285–290.

Otsu, N. (1979). A threshold selection method from gray-level histograms. IEEE Trans. Syst. Man Cybern. *9*, 62–66.

Pearson, K. (1901). On lines and planes of closest fit to systems of points in space. Philos. Mag. *2*, 559–572.

Potti, A., Dressman, H.K., Bild, A., Riedel, R.F., Chan, G., Sayer, R., Cragun, J., Cottrill, H., Kelley, M.J., Petersen, R., et al. (2006). Genomic signatures to guide the use of chemotherapeutics. Nat. Med. *12*, 1294–1300.

Prill, R.J., Iglesias, P.A., and Levchenko, A. (2005). Dynamic properties of network motifs contribute to biological network organization. PLoS Biol. *3*, e343.

Sigal, A., Milo, R., Cohen, A., Geva-Zatorsky, N., Klein, Y., Alaluf, I., Swerdlin, N., Perzov, N., Danon, T., Liron, Y., et al. (2006). Dynamic proteomics in individual human cells uncovers widespread cell-cycle dependence of nuclear proteins. Nat. Methods *3*, 525–531.

Sigal, A., Danon, T., Cohen, A., Milo, R., Geva-Zatorsky, N., Lustig, G., Liron, Y., Alon, U., and Perzov, N. (2007). Generation of a fluorescently labeled endogenous protein library in living human cells. Nat. Protoc. *2*, 1515–1527.

Strogatz, S.H. (2001). Nonlinear Dynamics and Chaos: With Applications to Physics, Biology, Chemistry, and Engineering (Cambridge, MA: Westview Press).

Tegner, J., Yeung, M.K., Hasty, J., and Collins, J.J. (2003). Reverse engineering gene networks: integrating genetic perturbations with dynamical modeling. Proc. Natl. Acad. Sci. USA *100*, 5944–5949.

Thattai, M., and van Oudenaarden, A. (2001). Intrinsic noise in gene regulatory networks. Proc. Natl. Acad. Sci. USA *98*, 8614–8619.

Yeh, P., Tschumi, A.I., and Kishony, R. (2006). Functional classification of drugs by properties of their pairwise interactions. Nat. Genet. *38*, 489–494.

Zhang, S.Z., Lipsky, M.M., Trump, B.F., and Hsu, I.C. (1990). Neutral red (NR) assay for cell viability and xenobiotic-induced cytotoxicity in primary cultures of human and rat hepatocytes. Cell Biol. Toxicol. *6*, 219–234.

Extended Results

Shuffling Tests Indicate that the Linear Superposition Is Statistically Significant

To test the significance of the linear superposition we performed two statistical tests. In the first test we calculated the Root Mean Square (RMS) error between the measured protein response to drugs combination and the best fit calculated superposition. In the second test we performed Principal Component Analysis (PCA) (Pearson, 1901; Jolliffe, 2002) on the measured protein response to the single drugs and to the drugs combination. PCA provides three eigenvalues (since there are three curves, 2 for single drugs and one for the combination). We calculated the smallest eigenvalue, which is an indication for the quality of the superposition (eigenvalues are normalized to sum up to one). If the smallest eigenvalue is zero it means that one of the measured responses (single or combined drugs) is a pure linear superposition of the other responses. High eigenvalue means that the measured responses (single or combined drugs) show some linear independence from each other.

For both RMS and PCA measures, we performed a data shuffling test. We compared the original dataset, in which the single drug response and the drugs combination response are for the same protein, to a randomly shuffled datasets in which the single drug responses are randomly chosen from other proteins (the drugs are not shuffled).

We performed 10,000 data shuffles (Figure S1). The original dataset is marked by a red circle in Figures S1A–S1F, and the shuffled tests are shown by the blue histogram. In all tested cases the original dataset is the absolute minimum of the RMS measure, and is distanced at least four standard deviations from the mean of the distribution (estimated P-value is $p < 10^{-4}$). In the PCA test the original dataset is the absolute minimum in the NCZ-CPT combination, but in the CPT-CisPt combination there are a few other combinations that show similar quality (estimated P-value is $p < 3 \cdot 10^{-2}$). This is probably because the measurements in these experiments are noisier.

Both tests show that the goodness of fit of linear superposition is statistically significant, and that dynamics of a given protein can not be explained by the dynamics of other proteins using linear superposition.

Control for Superposition: The Linear Superposition Is Not Explained by a Single Dominant Drug; the Sub-dominant Drug Is Also Important

We sought to control for the possibility that when one of the two drugs in a combination dominates the dynamics, linear superposition is less significant. In this case, the other, sub-dominant drug has a low weight. Therefore, as a control, we estimated the importance of the dynamics under the sub-dominant drug. We chose the experiment using CPT(0.33 μM)-NCZ(1 μM), since at these concentrations, CPT shows dominance over NCZ for most proteins. We used the RMS shuffling measure where now instead of shuffling both proteins, we shuffled only the protein for the sub-dominant drug NCZ, and left the original protein with its CPT response (Figure S1G). The RMS shuffling test shows that the dynamics in the sub-dominant drug NCZ is important to the linear superposition, and shuffling of the response to NCZ significantly effects the superposition.

Weights Are Not Strongly Correlated to the Amplitude of the Protein Response to Drugs

We also tested the relationship between the amplitude of protein response under a drug combination, and the weights it receives in the linear superposition. The response of a protein was measured by its RMS dynamics (a response of zero means the protein levels are unchanged by the drug combination relative to the level at the time of drug addition). The response in the combination was normalized by the response in each drug alone. We found no strong correlation between the linear superposition weights and the amplitude of the protein response.

Linear Superposition in a Protein Whose Dynamics Is Almost Unaffected by a Pair of Drugs

We studied a protein which had almost zero response to two drugs- the protein TOP1 under the drugs ETOPO (100 μM) and CisPt (80 μM). In this case, linear superposition (with any weights) would predict that TOP1 would also have almost zero response to the drug combination. This is indeed observed (Figure S2D).

Derivation of the Prediction Equations for Three and More Drugs

According to the linear superposition principle, we can write the equation for three drugs combination as:

$$P_{i+j+k} = w_i^{(ijk)} P_i + w_j^{(ijk)} P_j + w_k^{(ijk)} P_k \tag{1}$$

where P_i, P_j and P_k are the single drug responses, P_{i+j+k} is three drugs combination response and $w_i^{(ijk)}$ is the relative weight of one of the drugs. Our goal is to find an equation that predicts the weights $w_i^{(ijk)}$ based on the weights derived from a two-drug combination ($w_i^{(ij)}$).

According to the linear superposition principle, the two drugs combination can be written as:

$$\begin{aligned} P_{i+j} &= w_i^{(ij)} P_i + w_j^{(ij)} P_j \\ P_{i+k} &= w_i^{(jk)} P_i + w_k^{(ik)} P_k \\ P_{j+k} &= w_i^{(jk)} P_j + w_k^{(jk)} P_k \end{aligned} \tag{2}$$

Assuming that the weights are normalized to one: $w_i^{(ijk)} + w_j^{(ijk)} + w_k^{(ijk)} = 1$ and that the single drug responses are independent, we can write:

$$P_{i+j+k} = \left(1 - w_k^{(ijk)}\right) P_{i+j} + w_k^{(ijk)} P_k = \left(1 - w_j^{(ijk)}\right) P_{i+k} + w_j^{(ijk)} P_j = \left(1 - w_j^{(ijk)}\right) P_{j+k} + w_j^{(ijk)} P_i \tag{3}$$

comparing Equation (3) to Equation (1) we can extract 6 equations:

$$
\begin{aligned}
w_i^{(ijk)} &= \left(1 - w_k^{(ijk)}\right) w_i^{(ij)} = \left(1 - w_j^{(ijk)}\right) w_i^{(ik)} \\
w_j^{(ijk)} &= \left(\left(1 - w_k^{(ijk)}\right) w_j^{(ij)} = \left(1 - w_i^{(ijk)}\right) w_j^{(jk)} \\
w_k^{(ijk)} &= \left(\left(1 - w_i^{(ijk)}\right) w_k^{(jk)} = \left(1 - w_j^{(ijk)}\right) w_k^{(ik)}
\end{aligned}
\tag{4}
$$

which we can solve and extract the weights in the three-drugs combinations as a function of the weights in the two-drug combination:

$$
\begin{aligned}
w_i^{(ijk)} &= \frac{w_i^{(ik)} - w_i^{(ik)} w_j^{(jk)}}{1 - w_i^{(ik)} w_j^{(jk)}} = \frac{w_i^{(ij)} - w_i^{(ij)} w_k^{(jk)}}{1 - w_i^{(ij)} w_k^{(jk)}} \\
w_j^{(ijk)} &= \frac{w_j^{(jk)} - w_j^{(jk)} w_i^{(ik)}}{1 - w_j^{(jk)} w_i^{(ik)}} = \frac{w_j^{(ij)} - w_j^{(ij)} w_k^{(ik)}}{1 - w_j^{(ij)} w_k^{(ik)}} \\
w_k^{(ijk)} &= \frac{w_k^{(ik)} - w_k^{(ik)} w_j^{(ij)}}{1 - w_k^{(ik)} w_j^{(ij)}} = \frac{w_k^{(jk)} - w_k^{(jk)} w_i^{(ij)}}{1 - w_k^{(jk)} w_i^{(ij)}}
\end{aligned}
\tag{5}
$$

Using similar formalizes one can extract the general equation for predicting weights in multi-drug combinations as a function of the two drugs combinations:

$$
w_i^{(1..N)} = \frac{w_i^{(\neq j)} - w_i^{(\neq j)} w_j^{(\neq i)}}{1 - w_i^{(\neq j)} w_j^{(\neq i)}},
$$

where ($\neq j$) means all drugs but j.

The Mean Sum of Weights Is Correlated with the Antagonism-Synergism in Drug Combinations

We studied the relation between the superposition weights and the measured synergism-antagonism of drug combinations on cell killing. Figure S6 shows the correlation between the sum of weights averaged over all proteins and the measured synergism of the drug combination. The synergism of a drug combination is calculated by comparing the predicted viability of cells (fraction of surviving cells) after drug addition (V_{pre}) to the measured viability (V_{comb}). The predicted cell viability is calculated according to Bliss independence: $V_{pre} = V_1 \cdot V_2$ where V_1 and V_2 are viability after the addition of the individual drugs. Synergism is defined as V_{pre}-V_{comb}, where a positive synergism is when the predicted viability is higher than measured (the actual number of dead cells is higher than predicted), and a negative synergism (referred as antagonism) is when the actual number of dead cells is lower than predicted. The correlation between the mean sum of weights and synergism of killing, as shown in Figure S6, is quite good with a correlation coefficient of $R^2 = 0.6$ (p $= 2\cdot10^{-4}$).

Why should weight sum correlate with synergy? Intuitively, if weights sum to more than one, the response with two drugs is more than the average of the responses of each drug alone. If protein responses carry the biological outcome (cell killing in the present case), such high weight sum may correlate with synergy. Conversely, sum of weights smaller than one means responses less than the average of single drug dynamics, and intuitively may correspond to antagonism.

Cyclic Dominance of Drugs—The Case of DDX18

The response of DDX18 shows a cyclic dominance of drugs, an unusual situation. In the response of DDX18, NCZ dominates CPT which dominates CisPt which dominates NCZ. A possible hypothesis is that in the case of DDX18 there is an interaction between the drugs in which the response to one of the drugs is silenced: NCZ silences CPT, CPT silences CisPt and CisPt silences NCZ. We used the following to find a good estimate of the measured weight: DDX18 weight in the combination of NCZ-CisPt is 1 for CisPt and 0 for NCZ, and in the combination of CPT-CisPt it is 1 for CPT and 0 for CisPt.

Adding a Drug to Itself

An interesting case is when a drug is added to itself, which can be considered as a limiting case in which the two drugs in a cocktail are one and the same. Linear superposition of a drug with itself means that the dynamics in dose D_1+D_2 is a weighted sum of the dynamics in D_1 and D_2:

$$
P(D_1 + D_2, t) = w_1 \cdot P(D_1, t) + w_2 \cdot P(D_2, t)
$$

Here, the dose and time dependent dynamics is denoted $P(D,t)$, where D is the dose.

We tested this experimentally with CPT, ETOPO and CisPt. We find good linear superposition for the concentrations tested (Table S1, Figure S5).

Dynamics in Drug with Itself Is a Linear Superposition of the Dynamics in Each Drug Alone

One can show that linear superposition applies provided that the dose-dependent dynamics has a certain mathematical feature, called separability. To defined separability, note that at zero dose, one finds a basal dynamics *P(0,t)*. At high doses, the dynamics usually saturates to a limiting profile *P(∞,t)*. If the profile at intermediate doses moves smoothly between these two limiting profiles, such that:

$$P(D, t) = P(0, t) + (P(\infty, t) - P(0, t)) . g(D),$$

we say the drugs response is separable. That is, the transition between the zero drug profile and saturating drug profiles depends on dose through a function g(D) that does not depend on time.

A drug with separable dynamics shows linear superposition, because

$$P(D_1 + D_2, t) = w_1 \cdot P(D_1, t) + w_2 \cdot P(D_2, t)$$

Plugging in weights that sum up to one, $w_1 + w_2 = 1$, results in

$$w_1 = \frac{g(D_1 + D_2) - g(D_2)}{g(D_1) - g(D_2)}$$

$$w_2 = \frac{g(D_1 + D_2) - g(D_1)}{g(D_2) - g(D_1)}$$

These weights can be negative and the case $D_1 = D_2$ is a singular. Other solutions are possible with weights that do not sum to one as well.

It is possible to conceive a case where dynamics does not show separability, for example when *P(D,t) = D/(K(t)+D)* with a time dependent *K(t)*. It would be interesting to investigate other drugs for self-superposition. See Figure S5.
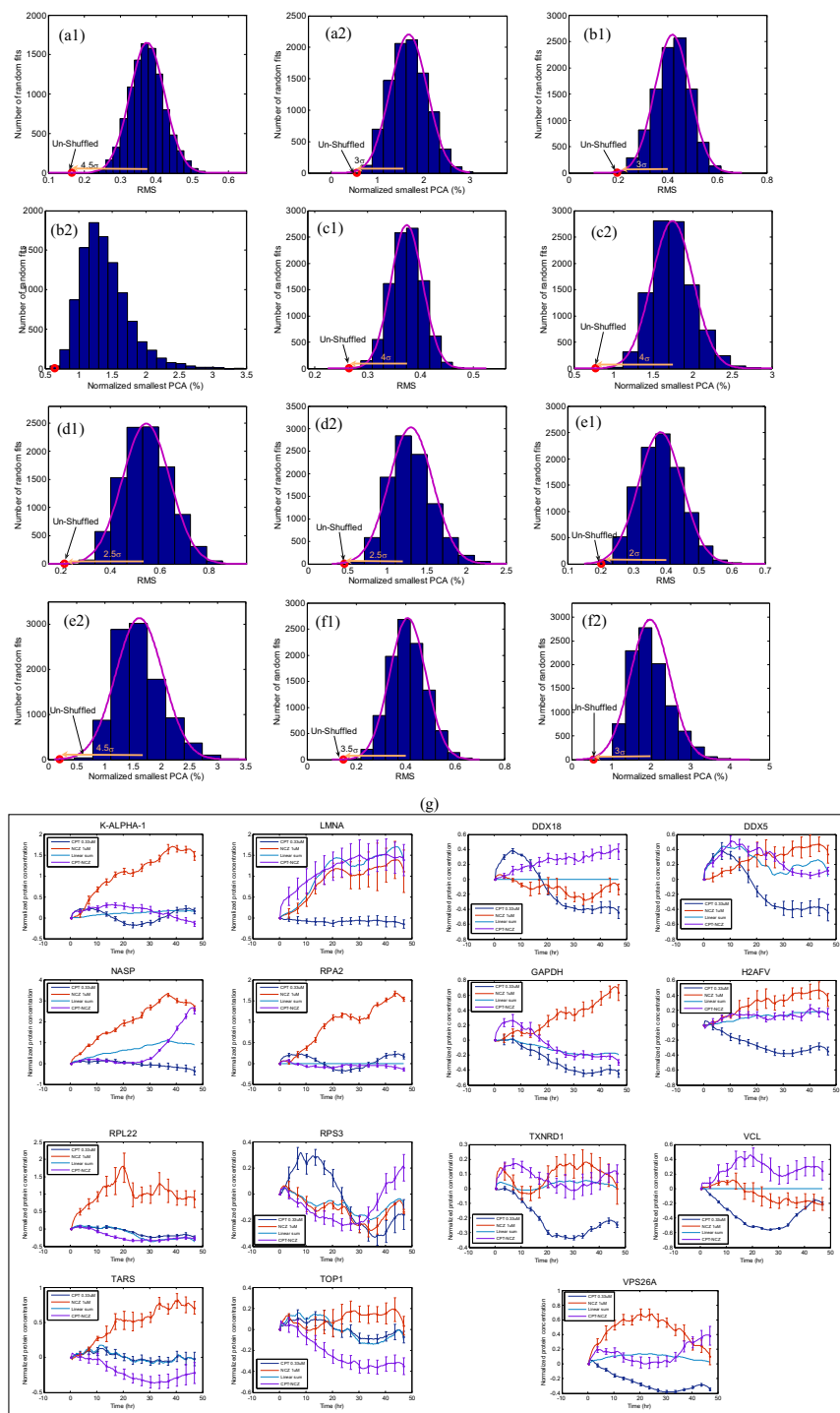
Figure S1. Significance of the Linear Superposition, Related to Figure 2

(A–F) Shown by two methods for CPT(0.33 μM) – NCZ(1 μM) drugs combination (A), for CPT(0.33 μM) -CisPt(80 μM) drugs combination (B), for NCZ(1 μM) – CisPt(80 μM) drugs combination (C), for CPT(0.33 μM) – ETOPO(100 μM) drugs combination (D), for NCZ(1 μM) – ETOPO(100 μM) drugs combination (E), and for CisPt(80 μM) – ETOPO(100 μM) drugs combination (F) . (1) The RMS (Root Mean Square) between the best-fit linear superposition and the measured protein response to CPT and NCZ. The smaller the RMS values the closer are the measured and calculated protein responses. (2) The smallest eigenvalue of a PCA (Principal Component Analysis) applied to the single and combined drugs responses (in percent of the sum of eigenvalues). Small relative values of this eigenvalue means that the measured two drugs combination response is close to a linear superposition of single drug dynamics. The red circle is the original dataset where the protein in the drug combination is matched to its own individual drug response. Blue histogram is for random shuffling where a drug combination is matched

with the single drug responses of randomly chosen proteins. In both methods the original dataset is the absolute minimum. The magenta line is a fit of the distribution to a normal distribution. The original data set is 4.5 standard deviations (σ) from the mean of the distribution in the RMS measure and 3σ from the mean of the distribution in the PCA measure, meaning that the linear superposition is statistically significant ($p < 2 \cdot 10^{-3}$).

(G) Dynamics in CPT(0.33 μM) - NCZ(1 μM) drugs pair when individual drug responses are randomly shuffled does show a linear superposition of the dynamics of each drug alone. Shown are protein dynamics of the individual drugs: blue line is for CPT(0.33 μM), red line is for NCZ(1 μM) randomly chosen from other proteins, purple is for the combination of the two drugs and light blue is the best fit linear superposition.

Error bars are standard errors of 3 or more independent experimental repeats.
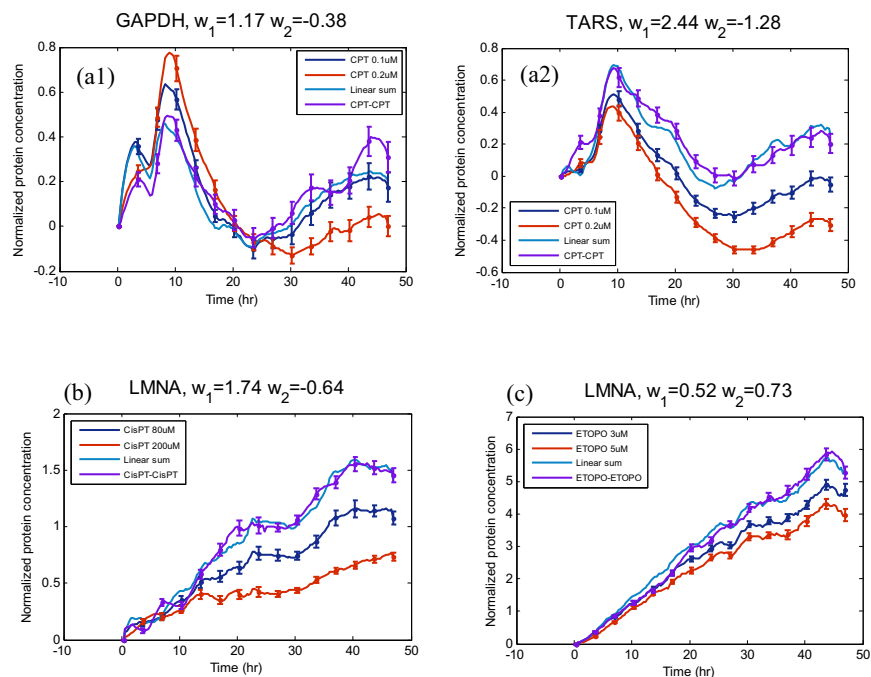
Figure S2. Dynamics in Drug with Itself Is a Linear Superposition of the Dynamics in Each Drug Alone, Related to Figure 2

Shown are protein dynamics of the individual drugs.

(A) Blue line is for CPT (0.1 μM), red line is for CPT (0.2 μM) purple is for CPT (0.3 μM) and light blue is the calculated linear superposition. The weights are indicated at the title.

(B) Blue line is for CisPt (80 μM), red line is for CisPt (200 μM) purple is for CisPt (280 μM) and light blue is the calculated linear superposition. The weights are indicated in the title.

(C) Blue line is for ETOPO (3 μM), red line is for ETOPO (5 μM) purple is for ETOPO (8 μM) and light blue is the calculated linear superposition. The weights are indicated in the title.

Error bars are standard errors of 3 or more independent experimental repeats.
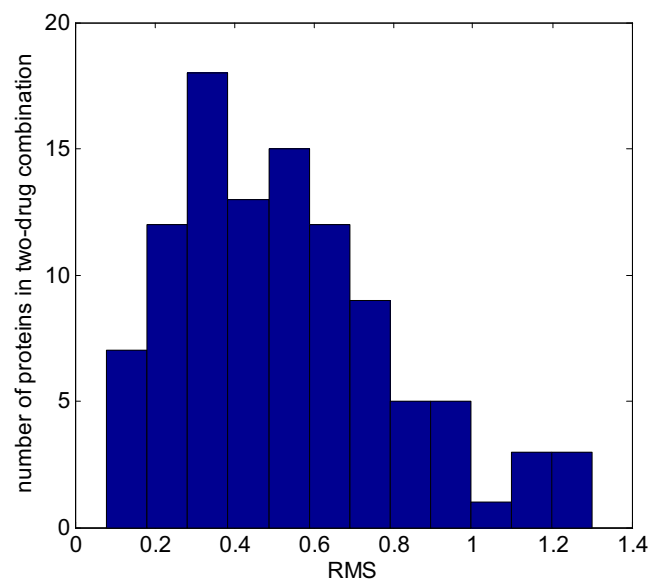
Figure S3. Histogram of all RMS Values in Two-Drug Combinations, Related to Figures 2 and 3
Shown are RMS values (summarized from Table S2) in two-drug combinations dynamics for all tested proteins.
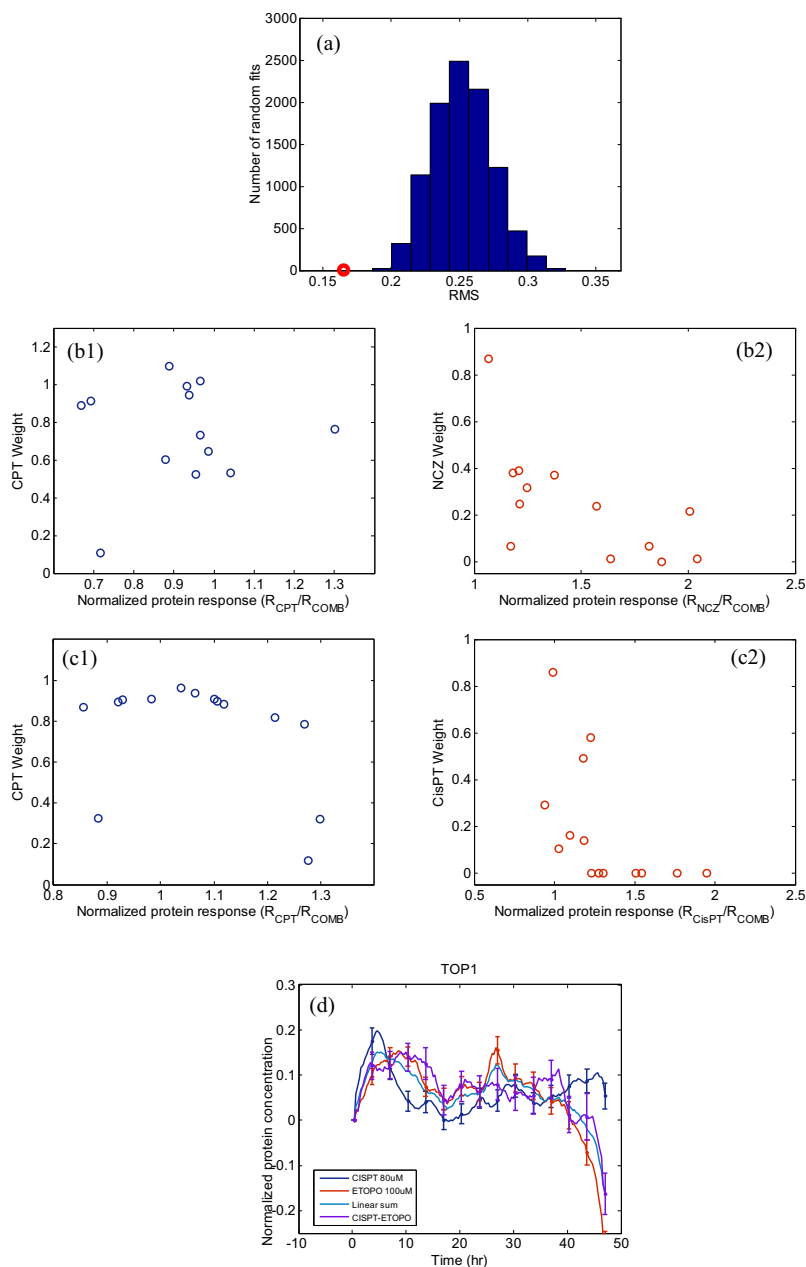
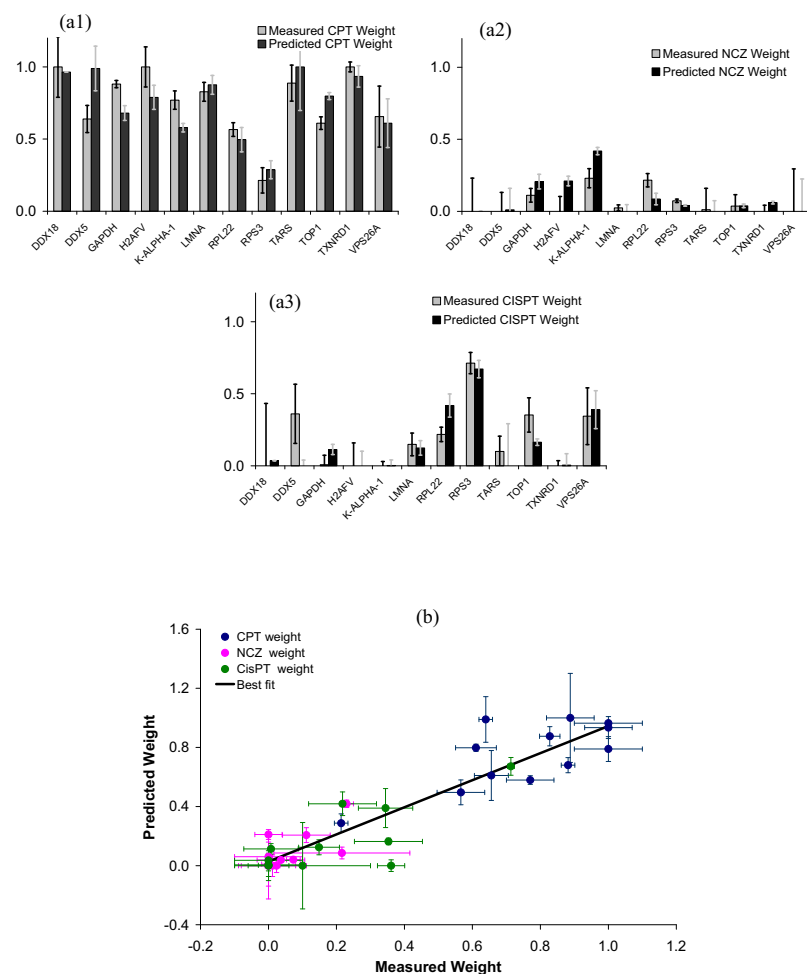**Figure S4. Related to Figure 3**

(A) Significance of the sub-dominant drug in the linear superposition is shown by shuffling the protein dynamics for the sub-dominant drug alone. Shown is a histogram of the RMS (Root Mean Square) between the calculated linear superposition and the measured protein response to the combination of CPT and NCZ. The histogram is for random shuffling of the response to the sub-dominant drug (NCZ) alone. Note that this test has increased significance, due to the smaller disturbance made by the sub-dominant drug shuffled data.

(B) Weights are not strongly correlated to the degree to which a protein responds to the drugs. Shown are the best fitted weights of (1) CPT and (2) NCZ in the linear superposition against the normalized protein response (R_{CPT}/R_{COMB} and R_{NCZ}/R_{COMB}). R_{CPT} and R_{NCZ} is the mean root square of the protein response to CPT or NCZ respectively and R_{COMB} is the mean root square of the protein response to the combination of CPT and NCZ. In this plot the response is also normalized to 1 at time $t = 0$.

(C) High weights are not usually assigned to low response. Shown are the best fitted weights of (1) CPT and (2) CisPt in the linear superposition against the normalized protein response (R_{CPT}/R_{COMB} and R_{CisPt}/R_{COMB}). R_{CPT} and R_{CisPt} is the mean root square of the protein response to CPT or CisPt respectively and R_{COMB} is the mean root square of the protein response to the combination of CPT and CisPt. In this plot the response is also normalized to 1 at time $t = 0$.

(D) Linear superposition in a case where the two drugs cause an almost zero response of the protein. TOP1 dynamics in response to CisPt (80 μM), (blue), ETOPO (100 μM), (red), the combination CisPt (80 μM) – ETOPO (100 μM), (purple) and the calculated linear superposition (light blue).

Error bars are standard errors of 3 or more independent experimental repeats.

Figure S5. Related to Figures 3 and 5

(A) Dynamics in a combination of three drugs is a linear superposition of single drug dynamics, and can be predicted based on two-drug weights. Measured and predicted weights of CPT (1), NCZ (2) and CisPt (3) for the proteins. Error bars are confidence level of 95%.

(B) There is a good correlation between the predicted and measured weights of individual proteins. Shown are the weights of individual proteins in the three-drug combination CPT-NCZ-CisPt. The correlation coefficient is R = 0.92, and the P-value is $p = 5 \cdot 10^{-16}$. Error bars (x-axis) are confidence level of 95%, and (y-axis) are derived from our prediction equations (see the Extended Results) and 95% confidence of two-drug experiments.
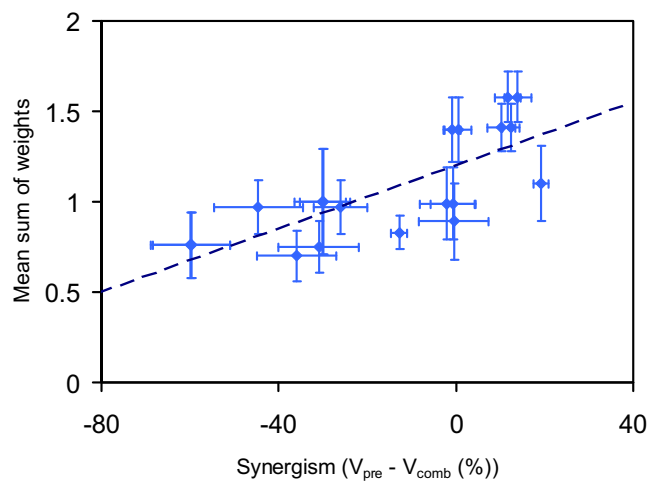
Figure S6. Synergism-Antagonism of Drug Combinations Correlates with Average Sum of Superposition Weights, Related to Table 1

Shown is the correlation between the measured synergism in viability tests (*x* axis, negative value indicate antagonism, positive value indicate synergism) and the mean sum of weights (un-normalized mean over individual proteins weights) of corresponding drug combination. We considered all experiments with two-, three- and four-drug combinations, at different drug doses. The correlation coefficient is $R^2 = 0.6$ with a P-value of $2 \cdot 10^{-4}$. Error bars are (x-axis) experimental standard errors and (y-axis) standard errors of weights.